

## Understanding Diffusion in Confined Systems: Methane in a ZK4 Molecular Sieve. A Molecular Dynamics Simulation Study

P. Demontis,\* L. A. Fenu, and G. B. Suffritti

Università di Sassari, Dipartimento di Chimica, Via Vienna 2, I-07100 Sassari, Italy

Received: May 17, 2005; In Final Form: July 29, 2005

The equilibrium probability distribution of  $N$  methane molecules adsorbed in the interior of  $n$   $\alpha$  cages of the ZK4 zeolite, the all-silica analogue of zeolite A, is modeled by a modified hypergeometric distribution where the effects of mutual exclusion between particles are extracted from long molecular dynamics simulations. The trajectories are then analyzed in terms of time-correlation functions for the fluctuations in the occupation number of the  $\alpha$  cages. The analysis digs out the correlations induced by the spatial distribution of the adsorbed molecules coupled with a migration mechanism where a molecule can pass from one  $\alpha$  cage to another, one-by-one. These correlations lead to cooperative motion, which manifests itself as a nonexponential decay of the correlators. Our results suggest ways of developing improved lattice approaches that may be useful for studying diffusion in much larger systems and for a much longer observation time.

Diffusion of adsorbed molecules is of paramount importance in catalysis and separation processes that take place in microporous materials. Recently, there has been a great deal of effort to simulate transport properties in zeolites.<sup>1–3</sup> These numerical models have advanced significantly the theoretical basis for the extremely rich class of phenomena exhibited by these systems such as single-file diffusion,<sup>4,5</sup> correlated cluster dynamics,<sup>6</sup> levitation effect,<sup>7</sup> and percolation.<sup>8</sup> Auerbach and co-workers<sup>9</sup> proposed a new analytical theory for activated diffusion in zeolites at finite loadings by replacing the crystal lattice with a three-dimensional Ising lattice of binding sites. Despite this novel result and deeper understanding, it is still proving to be difficult to use molecular theories and numerical simulations to develop a predictive analytical theory for diffusion in zeolites. A molecule adsorbed in the channels and cavities of zeolites is under constant control of its surrounding medium, which determines the energy landscape for the transport process. Increasing the number of sorbate molecules alters this energy landscape by introducing new and sometimes more effective paths for the diffusion. This phenomenology has been highlighted by the pulsed field gradient-NMR experiments by Kärger and Pfeifer.<sup>10</sup> Different molecules adsorbed in zeolites of different topologies have shown at least five different types of dependence of the self-diffusivity  $D_s$  of the sorbate on its concentration  $c$ . In a previous paper,<sup>11</sup> we investigated, by molecular dynamics (MD) simulations, how the sorbate loading controls the diffusion of methane, represented as spherically symmetric Lennard-Jones molecules, in a cation-free (not-yet-synthesized) Linde type A zeolite (see below). The number density of the adsorbed molecules was increased from 1 up to 15 methane molecules per cavity. We found that the sorbate loading strongly influences the diffusion mechanism by inducing a transition from an increasing to a decreasing mobility regime, thus, reproducing one of the experimentally observed behaviors. Skoulidas and Sholl<sup>12</sup> observed a similar behavior in MD simulations of CH<sub>4</sub> and Ar diffusing in siliceous ITQ-3, a zeolite with a cage structure akin to ZK4, the all-silica analogue of zeolite A. They ascribed the increase in  $D_s$  with loading because of collective effects of molecules adsorbed in neighboring cages

that act to reduce the energy barrier for molecules to hop between cages relative to the energy barrier encountered by an isolated molecule. At sufficiently high loadings, steric hindrance will offset this energetic change, resulting in a net decrease in the self-diffusivity. This analysis has been supported by two papers by Tunca and Ford<sup>13,14</sup> that used transition state theory (TST) formalism to obtain the escape rate of adsorbate molecules from an  $\alpha$  cage in the zeolite ZK4 as a function of loading. They<sup>15,16</sup> proposed a new hierarchical approach for the modeling of small molecules at nonzero concentrations in microporous materials. Kärger et al.<sup>17</sup> pointed out its restricted regime of applicability. Nonetheless, in their opinion, this approach seems promising in its direct treatment of many body effects. Their criticism has been overcome recently by papers from Beerdson et al.<sup>18</sup> and Dubbeldam et al.,<sup>19</sup> where an extension to TST yields a diffusivity in excellent agreement with that obtained by conventional MD simulations, expanding the range of accessible time scales significantly beyond currently available methods.

In this paper, we exploit the benefits of the methane in ZK4 system extensively studied by Fritzsche et al.<sup>20–26</sup> that allows studying diffusion in the time scale accessible to MD simulations. We hope to contribute to the understanding of some of the details of the transfer of molecules from one cage to a neighboring cage as a function of loading. In particular, we will focus on the properties of the distribution of methane in the cages of ZK4 at different loadings and how the dynamical behavior is related to the fluctuations in the average occupancy  $\langle N \rangle$  per  $\alpha$  cage of the CH<sub>4</sub> molecules. Relying on these observations, we will propose an analysis of the diffusion process on the basis of the time-correlation formalism, where the fluctuations in the number of molecules that occupy an  $\alpha$  cage are the relevant observable to be correlated. In microporous solids, the multiplicity of locally stable structures that occur on the potential energy surface is deeply modified by the insertion of a newly adsorbed molecule in the host cage.  $N$  molecules adsorbed in a zeolite of “free” volume  $V$  fix the energy landscape. The number of molecules per cage is then the relevant parameter, which determines the type of motion the molecules

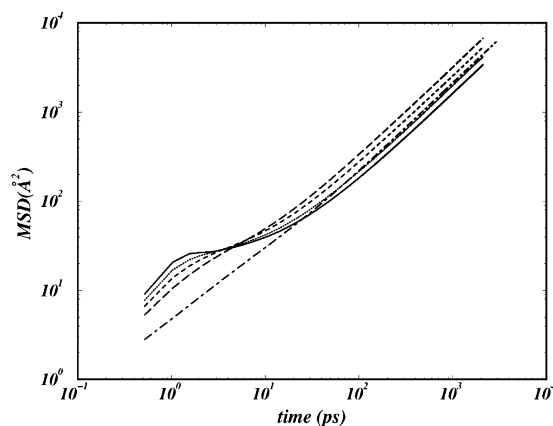


**Figure 1.** Log-log plot of the mean square displacement as a function of time. Continuous line,  $\langle N \rangle = 1$ ; dotted line,  $\langle N \rangle = 3$ ; dashed line,  $\langle N \rangle = 5$ ; long dashed line,  $\langle N \rangle = 7$ ; dot-dashed line,  $\langle N \rangle = 11$ .

are allowed to execute or, in other words, the space properties in which the molecules are confined.

Molecules adsorbed in the  $\alpha$  cage of ZK4 spend most of their time oscillating around the adsorption sites. In a previous paper,<sup>27</sup> four different regimes at different time scales were evidenced: quasi-free motion on a small time scale (up to 0.2 ps), oscillations about the preferred positions in the cavity (0.2–3 ps), intracavity diffusion (some tens of picoseconds), and long-range diffusion. In this last condition, the long-time motion of the adsorbed molecules can be treated as stochastic, as the time spent in each  $\alpha$  cage is long enough to cancel, to a great extent, any correlation with the past history of the migration dynamics. Thus, adsorbed molecules make a random walk between cages<sup>19</sup> whose properties may be very complicated by the presence of other molecules and the interactions with the surrounding walls of the cage.

### Model and Calculation Details

ZK4,<sup>28</sup> because of its symmetry and the relative simplicity of its framework constituents, is a convenient system in which to perform our computer experiments. It can be thought of as an ordered matrix that can trap clusters of molecules in its void space. Its crystal structure is a simple cubic array of nearly spherical cavities ( $\alpha$  cages) connected to six neighboring cavities by nearly circular windows of about 4.2 Å in diameter. Each cavity has an internal radius of about 5.7 Å and can host a maximum number of 16 methane molecules represented as soft Lennard-Jones spheres. One unit cell contains eight  $\alpha$  cages and consists of 192 Si and 384 O atoms represented in the  $Fm3c$ <sup>8</sup> space group ( $a = 24.555$  Å). We remark that, as a result of the absence of extraframework cations in the model lattice, all windows are free for diffusion. The interaction potentials used in our MD simulations performed in the microcanonical ensemble and other details about the properties of this kind of system have been extensively discussed.<sup>11,20–27</sup> Here, we only note that the mechanical flexibility of the framework allows for the energy relaxation of the adsorbed molecules that then act as an effective heat bath.<sup>29,30</sup> In this paper, we study a larger system consisting of  $2 \times 2 \times 2$  unit cells. This is the smallest system required to avoid any spurious periodic boundary conditions of the correlation effects in the cage-to-cage migration process.<sup>21</sup> So, our simulation box consists of 4608 atoms representative of the flexible zeolite framework plus the adsorbed methane molecules ranging from 64 to 704 in number. Each trajectory was at least 22 ns long, and the methane coordinates and velocities were stored every 512 fs. Here, we

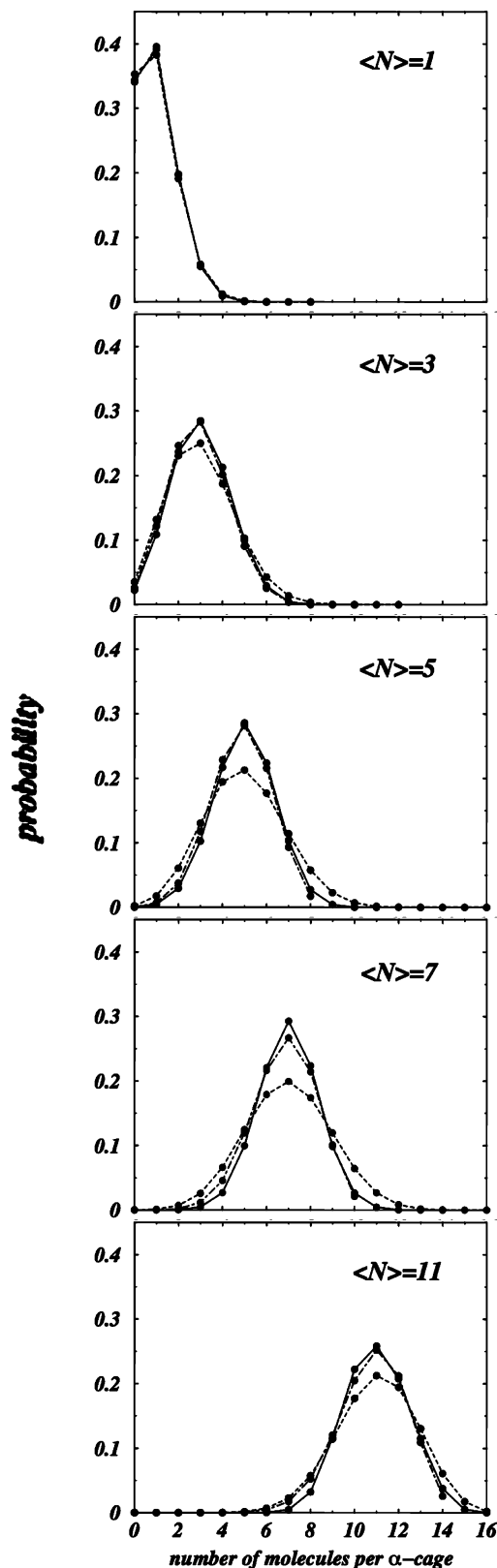


**Figure 2.** Probability distributions as a function of the number of molecules per  $\alpha$  cage. Solid lines are the simulation results. Dashed lines are calculated from the hypergeometric distribution (eq 3). Dot-dashed lines are calculated from the hypergeometric form (eq 3) with  $M$  obtained from eq 6 and by using the dispersions of the computed distributions.

consider some of the static and dynamical properties that can be extracted by sampling the system at different number densities (from 1, 3, 5, 7, and 11 molecules/cage) under the

nominal temperature of 360 K. The values of the self-diffusion coefficient  $D_s$  at various loadings are obtained from the Einstein relation<sup>31</sup>

$$D_s = \frac{1}{6} \lim_{t \rightarrow \infty} \frac{d}{dt} \langle |\mathbf{r}(t) - \mathbf{r}(0)|^2 \rangle \quad (1)$$

where the term in brackets is the mean-square displacement of the sorbed molecule. As reported in ref 11, the intercavity motion increases until the intracavity mobility is effective and the interparticle collisions assist the passing process to another cage. We observe a maximum in the  $D_s$  values at 7 molecules/cage. The mean-square displacement data are reported on logarithmic scales in Figure 1. Part of the phenomenology of the diffusive motion is captured by a power law of the form  $y = Ax^\alpha$ . The slope of any straight line fitting the data determines the power  $\alpha$ , while its height defines the factor  $A$ .<sup>32</sup> We note that a diffusive regime ( $\alpha = 1$  corresponding to  $\langle \Delta R^2 \rangle = D_s t$ ) is well-assessed for all the loadings considered here in a time domain between  $\sim 100$  and  $\sim 2000$  ps. Moreover, Figure 1 shows that the transition to the diffusive regime is sensitive going from low to high loading and that this is a signature of differences in the dynamics of cage migration. To illuminate this point, we determine the spatial distribution of the adsorbed molecules. First of all, we ask the following question: what is the probability of finding exactly  $N$  molecules within an  $\alpha$  cage? The answer to this question is given by the probability distribution of molecules over independent subvolumes,<sup>33</sup> a quantity that can be related to different interesting information about the system.<sup>34</sup> We look for a possible connection between these distributions and the cage-to-cage migration process. We use a distance criterion to decide whether a molecule belongs to a specific cage. A molecule within a distance of 6.1 Å from a cage center is assigned to the same examined cage. The ensemble average of these occupation numbers gives the curves reported in Figure 2. Following Velasco and co-workers,<sup>35</sup> we incorporated the effects of mutual exclusion between particles by a density-dependent effective volume per particle, which is related to the fluctuations in the cage particle number. For the sake of clarity, we briefly resume the method. For a perfect gas, composed of  $N_0$  point particles with no attractive forces, enclosed in a volume  $V_0$ , the probability of finding  $N$  particles in a subvolume  $V$  is given by the binomial distribution

$$W(N) = \binom{N_0}{N} p^N (1-p)^{N_0-N} \quad (2)$$

with  $p = V/V_0$ . Real molecules fill space, and so the probability of large values of  $N$  is reduced. Güémez et al.<sup>36,37</sup> solved this problem on the basis of the statistical problem of sampling without replacement. They supposed that the measure of the exclusion of additional molecules from a subvolume was proportional to the number already present. They showed that the distribution of finite-size particles among mutually exclusive lattice sites (lattice gas model) is given by the hypergeometric distribution

$$W(N) = \binom{N_0}{N} \binom{M-N_0}{K-N} \binom{M}{K} \quad (3)$$

where  $M$  and  $K$  are the number of lattice sites available in  $V_0$  and  $V$ , respectively, being  $K/M = V/V_0$ . This probability distribution is narrower than the binomial one; that is, fluctuations are suppressed by the property of mutual exclusion. It gives explicit expressions for the mean particle number

$$\langle N \rangle = N_0 \frac{K}{M} = N_0 \frac{V}{V_0} \quad (4)$$

and if we define the  $i$ th moment of the probability distribution as

$$w_i(\langle N \rangle) = \sum_{N=0}^K (N - \langle N \rangle)^i W(N) \quad (5)$$

we get for the dispersion

$$\begin{aligned} w_2 &= N_0 \frac{K}{M} \left( \frac{M-K}{M-1} \right) \left( 1 - \frac{N_0}{M} \right) \\ &= N_0 \frac{V}{V_0} \left( \frac{1 - \frac{V}{V_0}}{1 - \frac{1}{M}} \right) \left( 1 - \frac{N_0}{M} \right) \end{aligned} \quad (6)$$

that is an expression in terms of the relevant parameters characterizing the problem. In general, we expect a distribution function even narrower than the hypergeometric one, because the chance of finding space large enough to accommodate a methane molecule placed at random in an  $\alpha$  cage is less than the ratio  $M/K$  if the molecules are moving freely. The values of the dispersions  $w_2$  are obtained from our simulations so that an effective value of  $M$  is computed from eq 6. The distributions obtained by our MD runs are shown in Figure 2 and compared with that of the hypergeometric form (3) with  $M = 1024$  (the maximum number of sorption sites allowed in our simulation box is 64  $\alpha$  cages times a maximum of 16 sorption sites nominally allowed in each cage) and that of the hypergeometric form (3) with the effective values of  $M$ . The latter fits well with the observed distributions, which are narrower than the hypergeometric one, capturing the inefficient packing of methane guests in the confined  $\alpha$ -cage environments.<sup>38</sup> To highlight the local density fluctuations that occur within a given set of  $\alpha$  cages, we compare in Figure 3 the reduced variance  $(\langle N^2 \rangle - \langle N \rangle^2)/\langle N \rangle$  versus  $\langle N \rangle/N_{\max}$ <sup>39,40</sup> obtained from a strictly hypergeometric distribution of molecules among the cages and from our MD simulations. We observe a systematic deviation of our distributions from the hypergeometric ones. The less efficient packing of methane molecules in the  $\alpha$  cage is again well-evidenced, and we note that the reduced variance can be used as a measure of the effectiveness to accommodate a new molecule in the  $\alpha$  cage. In this context, it is appropriate to remember that the zeolitic framework allows the adsorbed molecules to move in a potential field of varying magnitude and sign. The molecules are localized by the repulsive part of this potential field, and the extent of this localization depends on the temperature and other thermodynamic variables. There is, therefore, no exact defined volume, and a strict statistical mechanical connection between the reduced variance and a local isothermal compressibility related to the occupancy fluctuations in the  $\alpha$  cage would be desirable but, unfortunately, difficult to assess.<sup>41</sup>

In Figure 4, the average values of  $\text{CH}_4\text{--CH}_4$ ,  $\text{O}_f\text{--CH}_4$ , and the negative of the kinetic energy are reported versus  $\langle N \rangle$ . The nominal temperature of 360 K is high compared with that of the average  $\text{CH}_4\text{--CH}_4$  interaction energy but is roughly one-half compared with that of the interaction of methane with the surface oxygens ( $\text{O}_f$ ), which is about 8.5 kJ mol<sup>-1</sup> in all the considered cases. We observe that, even in a system of some complexity like this, the statistical distribution of methane

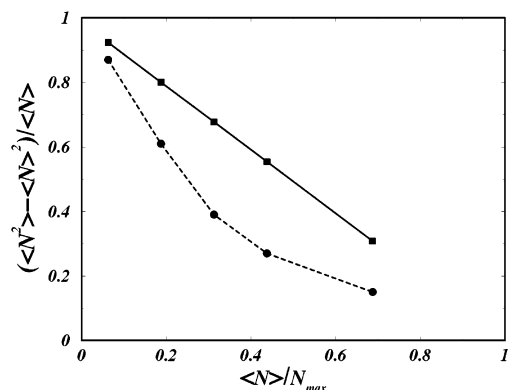


**Figure 3.** Reduced variance  $(\langle N^2 \rangle - \langle N \rangle^2)/\langle N \rangle$  vs  $\langle N \rangle/N_{\max}$  obtained from the strictly statistical hypergeometric distributions (square) which correspond to the 16 adsorption sites for methane molecules in the  $\alpha$  cages occupied under the rule of mutual exclusion and the distributions obtained from our MD simulations (circle).

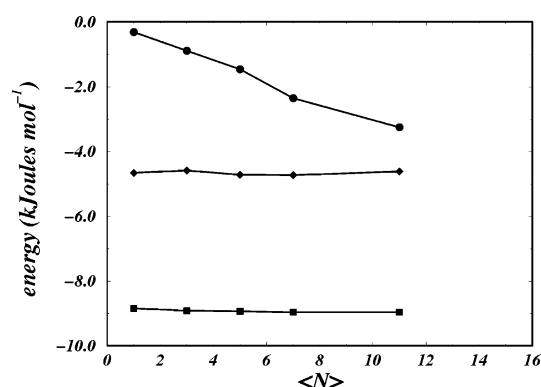


**Figure 4.** Circles, average values of the  $\text{CH}_4\text{--CH}_4$  potential energy; diamonds, average values of the negative of the kinetic energy; squares, average values of the  $\text{O}\text{--CH}_4$  potential energy reported vs  $\langle N \rangle$ .

molecules in the  $\alpha$  cages can be adequately described by a hypergeometric distribution by incorporating an effective value of  $M$ , at least when the temperature is high enough for the mutual repulsion of the adsorbed molecules to be the primary determinant of the distribution. Moreover, Figure 4 shows that the interaction between the methane molecules and the cage walls is to a large extent independent from the  $\text{CH}_4\text{--CH}_4$  interaction, which has a well-defined decreasing trend for all the considered values of  $\langle N \rangle$ . The  $\text{CH}_4\text{--CH}_4$  interaction is not modified by the interaction of methane with the surface oxygen that is responsible for the adsorption, but it does not influence the distribution of the molecules after the adsorption. This is, in our opinion, not always true depending on the nature of the interactions (which are only short-range Lennard-Jones in this case) and on the symmetry of the system under consideration (a simple cubic distribution of nearly spherical  $\alpha$  cages without charge-compensating ions in this case). In other words, in the case considered here, adsorption is not highly localized and the sorbate–sorbate interactions are comparable in strength to the sorbate–host interactions.

What we have learned so far is that molecules distribute themselves in the  $\alpha$  cages according to the mean distribution reported in Figure 2. This means that, at any instant of time, a specific cage can be occupied by a certain number of molecules, which can be different from its neighbors and from the value at the previous or following step. In Figure 5, we report the mean value of the cage residence time  $\tau_c$  calculated by using the same distance criterion used to assign a molecule to a given cage. We remark that cage-to-cage migration is a complex phenomenon<sup>11,20–27</sup> in which several factors can play a signifi-

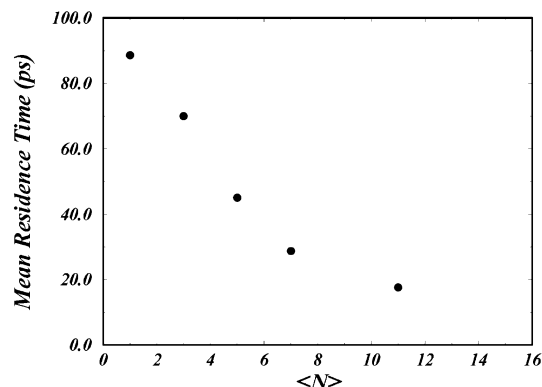


**Figure 5.** Mean residence time of a methane molecule in an  $\alpha$  cage as a function of loading  $\langle N \rangle$ .

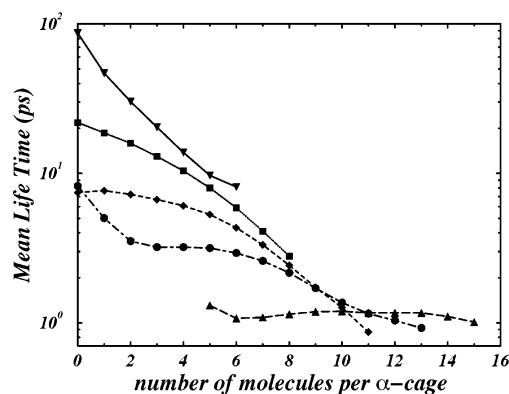


**Figure 6.** Mean lifetime of the number of molecules occupying each  $\alpha$  cage at the different loading  $\langle N \rangle$ . Triangle down,  $\langle N \rangle = 1$ ; square,  $\langle N \rangle = 3$ ; diamond,  $\langle N \rangle = 5$ ; circle,  $\langle N \rangle = 7$ ; triangle up,  $\langle N \rangle = 11$ .

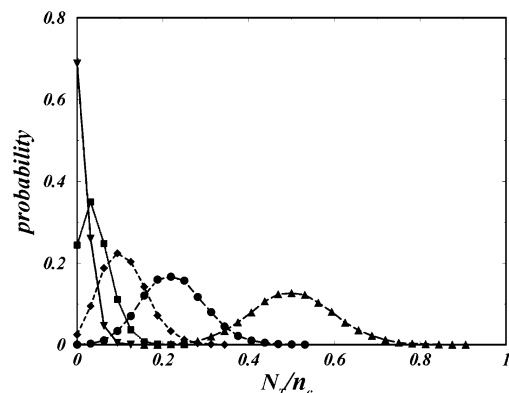


**Figure 7.** Probability distribution of  $N_T$  vs  $N_T/n_c$ .  $N_T(t) = \sum \Delta N_i(t)$ , total number of active transitions (see text). Triangle down,  $\langle N \rangle = 1$ ; square,  $\langle N \rangle = 3$ ; diamond,  $\langle N \rangle = 5$ ; circle,  $\langle N \rangle = 7$ ; triangle up,  $\langle N \rangle = 11$ .

cant role under specific conditions. The diffusion pathway of an adsorbed methane molecule from one cage to another neighboring cage implies the crossing of an eight-membered ring window. Its radius is about 2.1 Å; hence, methane molecules can pass from one  $\alpha$  cage to another, one-by-one. As we found in the smaller system,<sup>11</sup>  $\tau_c$  decreases with loading. We summarize the interpretation we gave of the microscopic dynamic in the smaller system that we think is still valid here. In a decreasing mobility regime, there is an increase in the probability that a molecule could visit the same cage many times despite a reduced value of  $\tau_c$ . For low loadings, the interactions between the sorbate molecules are less important and the energetic barriers for inter- and intracavity migration are roughly the same. Increasing the loading causes a reduction of the



**TABLE 1: Values of  $\Delta N_i(t) = |N_i(t + \Delta t) - N_i(t)|^a$** 

loading	$\Delta N_i(t) = 0$	$\Delta N_i(t) = 1$	$\Delta N_i(t) = 2$	$\Delta N_i(t) = 3$	$\Delta N_i(t) = 4$	$\Delta N_i(t) = 5$
1 ( $\sim 67$ ns)	8 291 738	96 607	198	1		
3 ( $\sim 22$ ns)	2 509 462	110 766	1078	6		
5 ( $\sim 22$ ns)	2 342 532	272 074	6634	70	2	
7 ( $\sim 22$ ns)	2 060 634	531 102	28 750	814	12	
11 ( $\sim 24$ ns)	1 614 098	1 101 592	156 384	10 980	394	8

<sup>a</sup> The absolute value of the difference in population between two subsequent stored instants of time observed during each trajectory (see text).

available adsorption sites, and the collisions between sorbed molecules become much more frequent. To supplement this picture of the migration process, we explore the mean lifetime of  $N$  (the number of molecules occupying each  $\alpha$  cage) at the different loading values,  $\langle N \rangle$ . Molecules going into or out of an  $\alpha$  cage will vary this quantity. These values are reported in Figure 6. We observe the following: (i) the curves cover 2 orders of magnitude on the time axis; (ii) a less-filled cage lives longer; (iii) an empty cage has, in general, the longest mean lifetime; (iv) at the higher  $\langle N \rangle$ , the curve is very flat; and (v) all of the curves follow a decreasing trend with increasing  $N$ . These curves clearly show that the migration dynamics are sensitive to  $\langle N \rangle$ . For example, if you look at  $N = 5$ , you find by inspection of Figure 6 a mean lifetime spanning from  $\sim 10$  to  $\sim 1$  ps. This gap progressively reduces going to a higher  $N$ . We propose a possible explanation that takes into account the probability distribution of molecules in the  $\alpha$  cages. In Figure 2 we have seen how molecules distribute themselves in ZK4. So, at each instant of time, a cage will have neighboring cages with an occupation number according to the proper<sup>42</sup> probability distribution. At low values of  $N$ , the mean lifetime is more sensitive at the occupation number of the neighboring cages while this effect becomes less important when  $N$  becomes high. In other words, when a cage is filled over a certain threshold, the probability to change  $N$  and the related mean lifetime seems to be less influenced by the occupation number of the neighboring cages. We remark that these effects are observed in the specific thermodynamic condition of our simulations, and to extract a more general trend, it will be necessary to put forth a much more extensive effort to explore different temperatures and loadings. We have seen that, at each instant of time, a generic cage  $i$  is populated by a number  $N_i(t)$  of methane molecules. We define the following quantities:  $\Delta N_i(t) = |N_i(t + \Delta t) - N_i(t)|$ , the absolute value of the difference in population between two subsequent stored instants of time ( $\Delta t \sim 0.5$  ps), and  $N_T(t) = \sum \Delta N_i(t)$ , the total number of active transitions or transitions which actually change the occupation number. We then calculate the probability distribution of  $N_T$  versus  $N_T/n_c$  ( $n_c = 64$ , the number of  $\alpha$  cages in our simulations) for each loading. The results are reported in Figure 7. We observe that the mean number of transitions per  $\alpha$  cage increases when the loading increases, and if we look at the value of the number of transitions per  $\alpha$  cage averaged along the trajectory, we find 0.01, 0.04, 0.11, 0.23, and 0.50 going from the lower to the higher loading, considered here in agreement with an observed decreasing mean residence time (see Figure 5). Table 1 reports the values of  $\Delta N_i(t)$  observed during each trajectory. We note that increasing the loading increases the probability of observing a value of  $\Delta N_i(t)$  greater than 1. This static picture needs to be accompanied with a dynamical description of the time evolution of the fluctuations in the  $\alpha$ -cage occupation numbers. Let  $\delta N(t) = N(t) - \langle N \rangle$  represent these fluctuations. The correlation between  $\delta N(t)$  and any spontaneous fluctuations at time zero that are migration

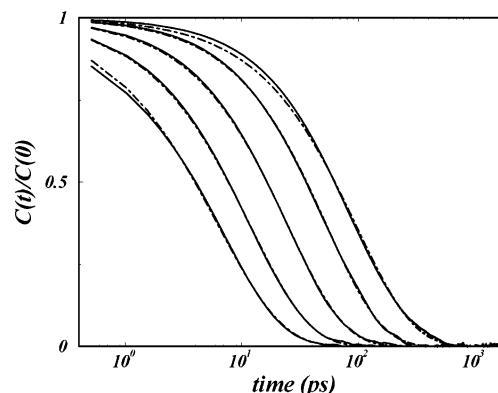


**Figure 8.** Temporal evolution of the normalized correlation function  $C(t)/C(0)$  for the different loadings considered in this paper. The solid curves correspond to the results of the simulations going from the higher value of loading (the inner curve) to the lower (the outer curve). The dot-dashed curves are fits to the data according to the Kohlrausch–Williams–Watts law (eq 7).

events into or out of the  $\alpha$  cage is  $C(t) = \langle \delta N(0) \delta N(t) \rangle = \langle N(0)N(t) \rangle - \langle N \rangle^2$ , with  $C(0) = \langle \delta N(0) \delta N(0) \rangle = \langle N^2 \rangle - \langle N \rangle^2$  as the variance.

In Figure 8, we report the normalized correlation function  $C(t)/C(0)$  for the different loadings considered in this paper. The solid curves correspond to the results of the simulations going from the higher value of loading (the inner curve) to the lower value (the outer curve). As can be seen, the entire dynamical behavior is observed in the time window of our simulations because the correlation functions decay to zero. We note that, for increasing loading, the decay of the correlation functions is faster. This confirms the previous considerations about the mean lifetimes and the probability to observe simultaneous transitions. The best fit of these correlation functions is obtained with a Kohlrausch–Williams–Watts law<sup>43,44</sup> or stretched exponential

$$C(t)/C(0) = \exp[-(t/\tau)^\beta], \quad 0 < \beta \leq 1 \quad (7)$$

The curves resulting from this fitting are shown in Figure 8 as dot-dashed lines. We note that there is very good agreement, especially for  $\langle N \rangle = 7, 5$ , and  $3$ . An evident deviation of our MD simulation results from eq 7 and is observable only in the heads of the correlators for  $\langle N \rangle = 11$  and  $\langle N \rangle = 1$ . Stretched exponential relaxations are the signature of cooperative motions. A reasonable conjecture for this finding is the model of hierarchically constrained dynamics, which implies triggering of slower relaxation processes after the completion of faster ones.<sup>45</sup> In a lattice model of the zeolite silicalite, Coppens et al.<sup>46</sup> observed, for the first time, a stretched exponential relaxation. In Figure 9, we report the collapse of correlators onto a single curve when plotted versus  $[t/\tau(\langle N \rangle)]^\beta$ . This is a noteworthy result that is generally ascribed to the existence of a scaling law, but before any final conclusions are drawn, further simulations and analyses are required; this will be the subject

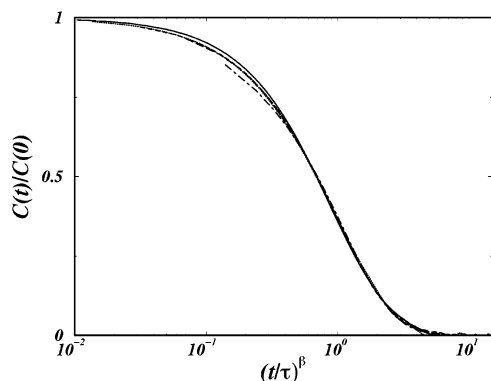


**Figure 9.** Evolution of the normalized correlation function  $C(t)/C(0)$  vs  $(t/\tau)^\beta$ . The correlators at different loadings collapse onto a single curve.

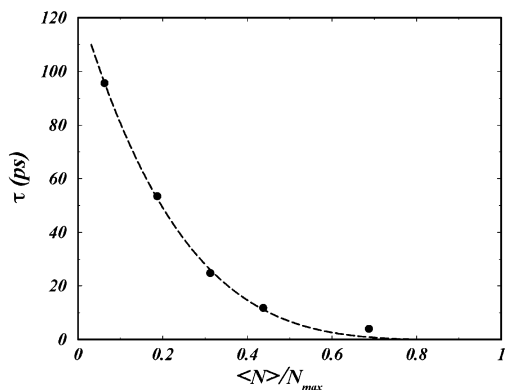


**Figure 10.** Relaxation time  $\tau$  vs  $\langle N \rangle/N_{\max}$ . The dashed curve is the best fit obtained from the equation  $\tau = c[1 - (\langle N \rangle/N_{\max})]^\gamma$ .

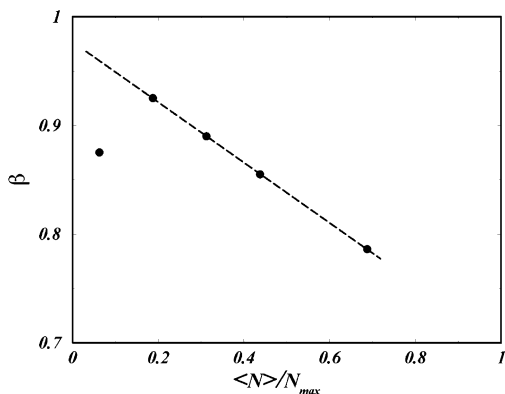


**Figure 11.** Values of  $\beta$  vs  $\langle N \rangle/N_{\max}$ . The dashed curve is the best fit of these data achieved in the range between  $\langle N \rangle = 3$  and  $\langle N \rangle = 11$  by the linear function  $\beta = a + b[1 - (\langle N \rangle/N_{\max})]$ .

of a forthcoming paper. The stretching exponent  $\beta$  has a value between 0.925 and 0.786, while the relaxation time  $\tau$  varies in the range between 95.6 and 6.3 ps. In Figure 10, we show the values of  $\tau$  versus  $\langle N \rangle/N_{\max}$ . We find that the best fit of these data is given by the function  $\tau = c[1 - (\langle N \rangle/N_{\max})]^\gamma$ . Our estimates yield  $c \approx 125.6$ ,  $\gamma \approx 4.2$ , and  $N_{\max} = 16$  that coincide with the maximum loading per  $\alpha$  cage at which a structural arrest in our system occurs. In Figure 11, we show the values of  $\beta$  versus  $\langle N \rangle/N_{\max}$ . We find that the best fit of these data is achieved in the range between  $\langle N \rangle = 3$  and  $\langle N \rangle = 11$  by the linear function  $\beta = a + b[1 - (\langle N \rangle/N_{\max})]$ . Our estimates yield  $a \approx 0.7$  and  $b \approx 0.28$ . We remark that the value at  $\langle N \rangle = 1$  does not fit the straight line, but at this moment, we do not have a clear-cut explanation of this behavior, which could probably be related to the mean lifetime of the number of

molecules occupying each  $\alpha$  cage, as reported in Figure 6. On the contrary, we infer that the value of  $\tau$  could be related to the mean residence time reported in Figure 5. This suggests a connection between a single-particle property and the fluctuations in the number of molecules occupying an  $\alpha$  cage. We have proven that the number of molecules in each  $\alpha$  cage is ruled by the modified hypergeometric distribution and is randomly distributed between 0 and  $N_{\max}$ . An elementary migration process could be described by the rate constant  $k_{mn}$  that is associated with the hop of a molecule leaving a cage containing a cluster of  $n$  molecules and appearing in a neighboring cage containing a cluster of  $m - 1$  molecules.<sup>47</sup> In our system, the different combinations of occupation numbers in the leaving and arriving cages give rise to an amount of  $16 \times 15 = 240$  possible values of  $k_{mn}$ . Depending on the loading and the temperature, some of these occupation numbers will be more frequent than others, and depending on the value of  $k_{mn}$ , they will contribute more or less to the total migration process. So, it is reasonable to accept a hierarchy in the processes determining the value of  $k_{mn}$  that is mirrored in the stretched exponential behavior of the correlators. Obviously, this is only a sound judgment in an effort to establish, if it exists, a theoretical link between the microscopic dynamics and the values of  $\beta$  as a function of loading.<sup>48</sup>

## Conclusions

In this paper, the equilibrium distribution of the  $\text{CH}_4$  molecules among the  $\alpha$  cages of the zeolite ZK4 has been computed directly by long trajectories of MD simulations ranging from low  $\text{CH}_4$  loading up to intermediate compared to that of saturation that, in this system, is achieved at 16 molecules per  $\alpha$  cage. At the maximum loading considered here (11 molecules per  $\alpha$  cage), diffusion is still a measurable property on the time scale covered by our simulations ( $\sim 22$  ns). As a first result, we find a very good agreement between our calculated distributions and a hypergeometric form, where the maximum number of available lattice sites is obtained by using the dispersions of the computed distributions. In this way, it is possible to unambiguously define the local density fluctuations on the length scale of an  $\alpha$  cage. At a given  $\langle N \rangle$ , the reduced variance provides information about the tendency to accept a new molecule in the  $\alpha$  cage. This could be interpreted to be like a rough estimate of a local microscopic compressibility that acts as a suitable order parameter to describe the transition to an ever more decreasing mobility regime, which is not possible to fully characterize at higher loading on the time window of our MD simulations.

Then, on the basis of an analysis of the results using a time-correlation formalism, we have shown how the description of local density fluctuations can help in the understanding of the complex behavior in systems of interacting particles in restricted geometries. In zeolites, the physical space is naturally divided into “cells” (cavities), each one associated with multifarious local minima in the potential energy surface. A proper use of the correlation of the fluctuations in the  $\alpha$ -cage occupation number can help in studying the hopping rate for particles confined in a cubic-symmetry zeolite. We found that these correlations lead to cooperative motion that manifests itself as a nonexponential decay of the time-correlation functions also in the low-loading regime. We observe that the ingredients to get this kind of dynamical behavior are confinement and distribution of occupancies, which are strictly related to connectivity, and with a migration mechanism where a molecule can pass from one  $\alpha$  cage to another, one-by-one. It is not obvious, however, how

to develop a microscopic theory with the ability to predict the values of the  $\beta$  exponents starting from the above remarks. Anyway, these results encourage us to extend the study of the phenomenology of the correlation function of the fluctuations in the occupation number of the cavities and channels to zeolitic systems of different topologies and by varying the temperature and loading. To our knowledge, this is the first time realistic off-lattice molecular simulations have shown that stretched exponential relaxation is a property observable in a large enough zeolitic system after a long enough observation time. Moreover, we have shown that the effects of the fluctuations in the number of molecules occupying a given  $\alpha$  cage give rise to an interesting and rich phenomenology. At the same time, the use of this observation suggests a coarse-graining procedure that extends the conceptual model of Tunca and Ford<sup>15</sup> by appealing and adapting the scheme of the integer-lattice gas automata.<sup>49</sup> In brief, the basic idea of this procedure consists of a mapping of the occupation numbers on a three-dimensional grid of lattice sites representative of the  $\alpha$  cages. Each lattice site is, therefore, characterized by this trivial degree of freedom that will be updated synchronously with all other sites according to a local evolutionary rule extracted from the atomistic simulation.<sup>50</sup>

**Acknowledgment.** This work has been carried out with financial support provided by Italian Ministero dell'Istruzione, dell'Università e della Ricerca, by Università degli Studi di Sassari, and by INSTM.

## References and Notes

- (1) Kärger, J.; Ruthven, D. M. *Diffusion in Zeolites and Other Microporous Solids*; John Wiley & Sons: New York, 1992.
- (2) Demontis, P.; Suffritti, G. B. *Chem. Rev.* **1997**, 97, 2845.
- (3) Keil, F. J.; Krishna, R.; Coppens, M.-O. *Rev. Chem. Eng.* **2000**, 16, 71.
- (4) Hahn, K.; Kärger, J.; Kukla, V. *Phys. Rev. Lett.* **1996**, 76, 2762.
- (5) Gupta, V.; Nivarthi, S. S.; Keffer, D.; McCormick, A. V.; Davis, H. T. *Science* **1996**, 274, 164.
- (6) Sholl, D. S.; Fichthorn, K. A. *Phys. Rev. Lett.* **1997**, 79, 3569.
- (7) Yashonath, S.; Santikary, P. J. *Phys. Chem.* **1994**, 98, 6368.
- (8) Keffer, D.; McCormick, A. V.; Davis, H. T. *J. Phys. Chem.* **1996**, 100, 967.
- (9) Saravanan, C.; Jousse, F.; Auerbach, S. M. *Phys. Rev. Lett.* **1998**, 80, 5754.
- (10) Kärger, J.; Pfeifer, H. *Zeolites* **1987**, 7, 90.
- (11) Demontis, P.; Suffritti, G. B. *J. Phys. Chem. B* **1997**, 101, 5789.
- (12) Skoulidas, A. I.; Sholl, D. S. *J. Phys. Chem. A* **2003**, 107, 10132.
- (13) Tunca, C.; Ford, D. M. *J. Chem. Phys.* **1999**, 111, 2751.
- (14) Tunca, C.; Ford, D. M. *J. Phys. Chem. B* **2002**, 106, 10982.
- (15) Tunca, C.; Ford, D. M. *Chem. Eng. Sci.* **2003**, 58, 3373.
- (16) Tunca, C.; Ford, D. M. *J. Chem. Phys.* **2004**, 120, 10763.
- (17) Kärger, J.; Vasenkov, S.; Auerbach, S. M. In *Handbook of Zeolite Science and Technology*; Auerbach, S. M., Carrado, K. A., Dutta, P. K., Eds.; Marcel Dekker: New York, 2003; Chapter 10.
- (18) Beerdse, E.; Smit, B.; Dubbeldam, D. *Phys. Rev. Lett.* **2004**, 93, 248301.
- (19) Dubbeldam, D.; Beerdse, E.; Vlugt, T. J. H.; Smit, B. *J. Chem. Phys.* **2005**, 122, 224712.
- (20) Fritzsche, S.; Haberlandt, R.; Kärger, J.; Pfeifer, H.; Wolfsberg, M. *Chem. Phys. Lett.* **1990**, 171, 109.
- (21) Fritzsche, S.; Haberlandt, R.; Kärger, J.; Pfeifer, H.; Heinzinger, K. *Chem. Phys. Lett.* **1992**, 198, 283.
- (22) Fritzsche, S.; Haberlandt, R.; Kärger, J.; Pfeifer, H.; Heinzinger, K. *Chem. Phys.* **1993**, 174, 229.
- (23) Fritzsche, S.; Haberlandt, R.; Kärger, J.; Pfeifer, H.; Heinzinger, K.; Wolfsberg, M. *Chem. Phys. Lett.* **1995**, 242, 361.
- (24) Fritzsche, S.; Haberlandt, R.; Hofmann, G.; Kärger, J.; Pfeifer, H.; Heinzinger, K.; Wolfsberg, M. *Chem. Phys. Lett.* **1997**, 265, 253.
- (25) Fritzsche, S.; Wolfsberg, M.; Haberlandt, R.; Demontis, P.; Suffritti, G. B.; Tilocca, A. *Chem. Phys. Lett.* **1998**, 296, 253.
- (26) Fritzsche, S.; Haberlandt, R.; Wolfsberg, M. *Chem. Phys.* **2000**, 253, 283.
- (27) Demontis, P.; Suffritti, G. B. *Chem. Phys. Lett.* **1994**, 223, 355.
- (28) Pluth, J. J.; Smith, J. V. *J. Am. Chem. Soc.* **1980**, 102, 4704.
- (29) Demontis, P.; Fois, E. S.; Suffritti, G. B.; Quartieri, S. *J. Phys. Chem.* **1990**, 94, 4329.
- (30) Suffritti, G. B.; Demontis, P.; Ciccotti, G. *J. Chem. Phys.* **2003**, 118, 3439.
- (31) McQuarrie, D. A. *Statistical Mechanics*; Harper & Row: New York, 1976.
- (32) El Amrani, S.; Kolb, M. *J. Chem. Phys.* **1993**, 98, 1509.
- (33) Rowlinson, J. S.; Woods, G. B. *Physica A* **1990**, 164, 117.
- (34) Cheung, T. T. P. *J. Phys. Chem.* **1993**, 97, 8993.
- (35) Román, F. L.; White, J. A.; Velasco, S. *Phys. Rev. E: Stat. Phys., Plasmas, Fluids, Relat. Interdiscip. Top.* **1996**, 53, 2360.
- (36) Güémez, J.; Velasco, S. *Am. J. Phys.* **1987**, 55, 154.
- (37) Güémez, J.; Velasco, S.; Hernández, A. C. *Physica A* **1988**, 152, 226.
- (38) Güémez, J.; Velasco, S.; Hernández, A. C. *Physica A* **1988**, 152, 243.
- (39) Chmelka, B. F.; Raftery, D.; McCormick, A. V. M.; de Menorval, L. C.; Levine, R. D.; Pines, A. *Phys. Rev. Lett.* **1991**, 66, 580.
- (40) See, for instance, Hansen, J. P.; McDonald, I. R. *Theory of Simple Liquids*, 2nd ed.; Academic Press: London, 1986.
- (41) Truskett, T. M.; Torquato, S.; Debenedetti, P. G. *Phys. Rev. E: Stat. Phys., Plasmas, Fluids, Relat. Interdiscip. Top.* **1998**, 58, 7369.
- (42) Rowlinson, J. S. *J. Chem. Soc., Faraday Trans. 2* **1986**, 82, 1801 (Faraday Symposium 20).
- (43) Jameson, C. J. *Mol. Phys.* **2004**, 102, 723.
- (44) Kohlrausch, R. *Ann. Phys. (Leipzig)* **1847**, 12, 393.
- (45) Williams, G.; Watts, D. C. *Trans. Faraday Soc.* **1970**, 66, 80.
- (46) Palmer, R. G.; Stein, D. L.; Abrahams, E.; Anderson, P. W. *Phys. Rev. Lett.* **1984**, 53, 958.
- (47) Coppens, M.-O.; Bell, A. T.; Chakraborty, A. K. *Chem. Eng. Sci.* **1998**, 53, 2053.
- (48) Jameson, A. K.; Jameson, C. J.; Gerald, R. E., II. *J. Chem. Phys.* **1994**, 101, 1775.
- (49) Phillips, J. C. *Rep. Prog. Phys.* **1996**, 59, 1133.
- (50) Boghosian, B. M.; Yepez, J.; Alexander, F. J.; Margolus, N. H. *Phys. Rev. E: Stat. Phys., Plasmas, Fluids, Relat. Interdiscip. Top.* **1997**, 55, 4137.
- (51) Pazzona, F. G. Thesis. University of Sassari, Sassari, Italy, Laurea Degree in Chemistry, July 2005. Demontis, P.; Pazzona, F. G.; Suffritti, G. B. Submitted.